RESEARCH

Effect of doped Zn–PbI$_2$ nanostructures on structural and electrical properties of photodetector applications

Safaa Idan Mohammed[1] · Haider Mohammed Shanshool[1] · Khalil Ibraheem Imhan[1]

Abstract

The present study focuses on the structural and electrical properties of doped zinc–lead iodide (Zn–PbI$_2$) as-deposited film. Lead iodide (PbI$_2$) nanostructure was successfully prepared by thermal evaporation method on a glass substrate at room temperature. The analysis, characterization, and structural properties of PbI$_2$ were achieved using X-ray diffraction (XRD) and scanning electron microscopy. The PbI$_2$ was polycrystalline and had a hexagonal structure as proved using XRD. The measured values are in agreement with other experimental and theoretical data. Furthermore, the present research studied the effect of doping on the physical properties of lead iodide with zinc dopants at different weights (0.02, 0.04, 0.06, and 0.08) mg. The electrical properties of the fabricated metal–semiconductor–metal photodetector based on PbI$_2$ and Pb$_{1-x}$Zn$_x$I$_2$ layers prepared on glass substrates by thermal evaporation method were investigated. The obtained results of Schottky barrier heights for Pb$_{0.98}$Zn$_{0.02}$I$_2$ were significant. The current–voltage characteristics of the Pb$_{0.98}$Zn$_{0.02}$I$_2$ thin film have acted as a Schottky contact in dark and under white light, 460-nm light. The light responsivity has shown a peak at 460-nm chopped light. At a bias voltage of 1, 3, and 5 V, the photocurrent rise and decay times were investigated. The device has shown faster response times for 460-nm light. This fast response was attributed to the high quality of polycrystalline and showed a high quantum efficiency of 9.19×10^2% when it was illuminated by 460-nm light under the bias of 3 V.

Keywords Pb$_{1-x}$Zn$_x$I$_2$ nanostructures · *I–V* characteristics · MSM PD · Thermal evaporation method

Introduction

Lead iodide (PbI$_2$) is a wide bandgap semiconductor (Eg = 2.32 eV) and has been a semiconductor material for use in solid-state X-ray and gamma-ray detectors [1, 2]. The unit cell dimension is $a = 4{:}557$ and $c = 6{:}979$ Å [3]. Bhavsar et al. [4] studied thin films of Zn-doped and undoped lead iodide gel-grown crystals, by thermal evaporation method, and highly uniform thin films were obtained. Verma et al. [5] in another study synthesized the thin film of pure ZnO, Zn0.97Nd0.03O and Zn$_{0.97}$Sm$_{0.03}$O by using metallo-organic decomposition method. The average size of ZnO nanoparticles with Nd and Sm doping is 10 nm, confirmed with atomic force microscopy. The Nd and Sm doping into ZnO thin films significantly enhances absorption in the UV region and suggests its usability for UV detectors. Under UV irradiation ($l = 325$ nm), the value of photocurrent in Nd and Sm/ZnO thin films is highly enhanced for possible use in UV sensors. Lam et al. [6] in their study fabricated and characterized the ultraviolet (UV) photodetectors with ZnO nanorods (NRs)/Cds thin-film heterostructures on glass substrates. The study last comes to the conclusion that there is significantly high sensitivity in the range of UV light which can be useful for the application of UV detection. Bhardwaj et al. [7] in their study gave an explicit comparison on the basis of structure and electronic properties of ZnO nanostructures which were synthesized by sol–gel and hydrothermal method. Field-emission scanning electron microscopy revealed the formation of ZnO spherical nanoparticle structure for sol–gel method and flower like m-structure for ZnO prepared through hydrothermal route. Among the conclusions, they research into the idea that further extended X-ray absorption fine-structure revealed a similar local atomic structure for both samples despite having different morphologies. Some researchers have investigated the structural properties of PbI$_2$ [8, 9]. Because several methods for depositing films require sublimation or evaporation of

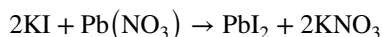✉ Safaa Idan Mohammed
safaadali431@gmail.com

1 Ministry of Science and Technology, Baghdad, Iraq

the material, it should have a temperature for appreciable evaporation or at least a temperature for appreciable sublimation as films that can be grown at temperatures lower than 250 °C, the maximum temperature for the detector stability during deposition. The material must be thick enough to absorb a high percentage of X-rays, taking into consideration its absorption coefficient. The grain size must be less than 100 μm, and therefore, small-grain-size polycrystalline films or epitaxial films are required [10]. In this work, the deposited film of doped Zn–PbI_2 with different weights of zinc dopants on the glass substrate was prepared successfully. The structural and electrical properties of samples were studied. To the best of the author's knowledge, the preparation of these samples with different weights of Zn dopant and studied their effect on electrical properties are considered to be the first work.

Experimental process

Lead iodide (PbI_2) powder preparation

Lead iodide (PbI_2) was prepared in the laboratory by the reaction of potassium iodide KI with lead nitrates $Pb(NO_3)_2$. In accordance with the following procedures, 1 mol/L of potassium iodide KI was dissolved in DI water at boiling temperature and vigorously stirred for 10 min. Same procedure was followed with 2 mol/L of lead nitrate $Pb(NO_3)_2$. After that, the two solutions were mixed in one beaker and placed on a hot plate at a temperature of boiling and stirred quickly for 1 h. (K) and (Pb) are the positive ions, while (I) and (NO_3) are the negative ions. The (NO_3) group is radical. We can observe from the sudden appearance of yellow precipitation that a chemical change has occurred. This proves the formation of PbI_2 crystalline in this solution. The positive charged (Pb) has combined with the negative charged I. Similarly, the K and (NO_3) group are combined. The equation describing the reaction may be written as follows:

$$2KI + Pb(NO_3) \rightarrow PbI_2 + 2KNO_3$$

Soon, a yellow deposit appeared at the bottom of the beaker. This deposit is the lead iodide (PbI_2), which is not soluble in water; while the potassium nitrates (KNO_3) are solved in water. Then, the water is removed from the beaker using a scaled syringe to avoid any disturbance may occur. After the deposited material is dried, it was removed from the bottom of the beaker and kept in desiccators.

Preparation of the thin-film samples

PbI_2 thin films were deposited on glass substrates at room temperature using electron beam evaporation (Auto 306 Vacuum Coater). The principal reason for using this technique

is to allow the deposition of a large area in a cost-effective manner [11]. Glass substrates were provided of thickness 1 mm and dimensions 15 × 20 mm prior to the thermal evaporation of PbI_2. Glass slides are often cleaned by a solvent clean, followed by a deionized water (DI) rinse, a mild acid clean, DI rinse, and blow-dry. It involves the following steps: Solvents can clean oils and organic residues which appear on glass surfaces by the following steps:
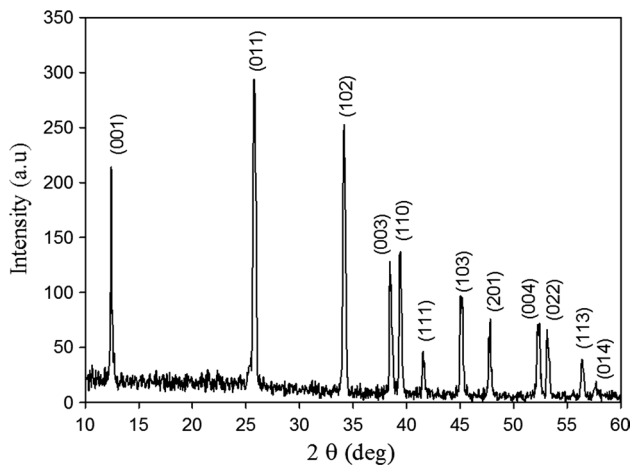
(a) Pour acetone into a glass container.
(b) Pour methanol in a separate container.
(c) Place acetone on a hot plate to warm up (do not exceed 55 °C).
(d) Place glass wafer in a warm acetone bath for 10 min.
(e) Remove and place in methanol for 2–5 min. Remove and rinse in DI water.
(f) Blow-dry with nitrogen.

The thermal evaporator deposits the metal onto the substrate. Under vacuum, the current passes through a filament which heats up the metal present in the boat. When the current reaches the evaporation value, the melted metal evaporates onto the substrate. This is done under high vacuum to allow the vapor to reach the substrate without reacting with or scattering against other gas-phase atoms in the chamber. $Pb_{1-x}Zn_xI_2$ nanostructure was deposited on a glass substrate using thermal evaporation under 5×10^{-5} torr vacuum. The contact as silver (Ag) mask was deposited via thermal evaporation on $Pb_{1-x}Zn_xI_2$ surface to create metallization grid patterns. First, the $Pb_{1-x}Zn_xI_2$ photodetector was annealed at 200 °C for 1/2 h to enhance the metal–semiconductor contact.
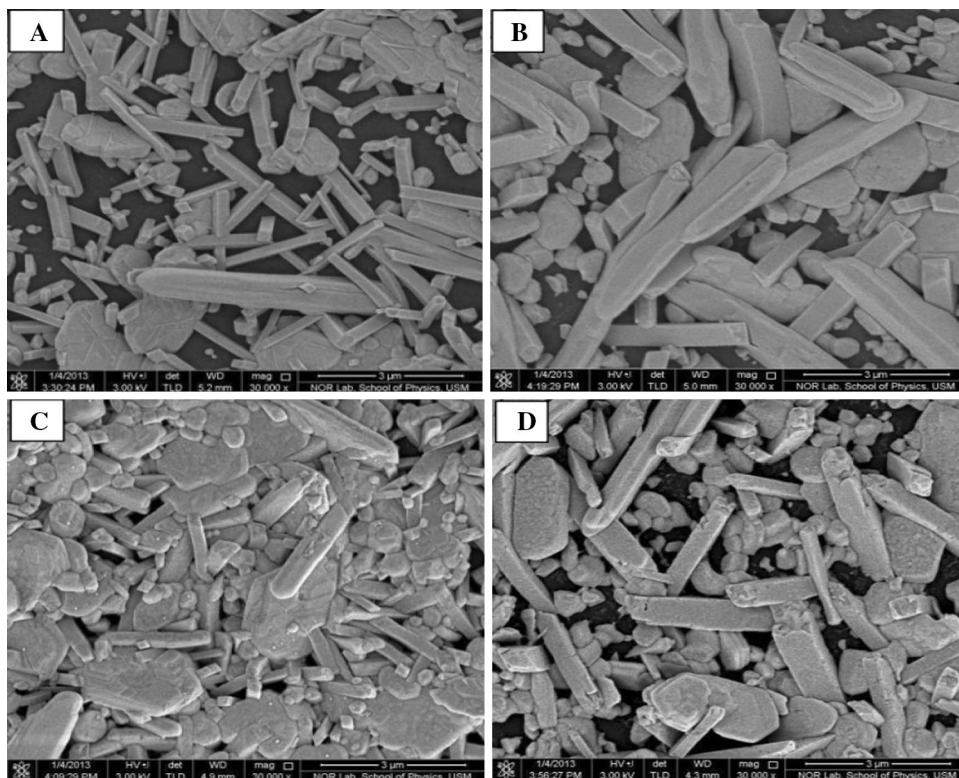
Characterization techniques

The weight method was adopted to measure the thickness. Sensitive electrical balance Metler AE-160 was used, with precision reaching 10^{-4} g. The structural properties of the deposited PbI_2 thin films were investigated by using X-ray diffraction to determine whether the sample is crystalline or not, also the diffraction is used to determine spacing, preferred orientation, and the average grain size. In our measurements, we used X-ray diffraction system (Philips PW 1710 X-ray diffractometer) with the following characteristics: source radiation of CuKα with 1.54 Å wavelength, incidence angle: 10°–60°, and scanning speed: (5°/min). The scanning electron microscope (SEM) images of these films were obtained by (SEM) model (JEOL-JSM-6460 LV). The energy bandgap from optical absorption is measured from Zn–PbI_2 thin films deposited on glass substrates using a UV–Vis spectroscopy. I–V characteristics are measured by (Keithley, 2400 system) high-voltage source. Two needle-like probes are positioned on

the contacts under voltage -5.0 to $+5.0$ V. It results in a current flow between the contacts which is measured via ammeter. These results are displayed on a screen or a monitor. The photo- and dark currents were taken into consideration. In addition, ideality factors and SBH depend on *I–V* measurements.

Results and discussion

XRD of PbI$_2$

Figure 1 shows the XRD pattern of the grown polycrystalline PbI$_2$. XRD pattern was obtained with scanning angles of $2\theta = 10°-60°$ for a high-purity PbI$_2$ crystal, containing the complete set of reflections. The sharp diffraction peak originates at $2\theta = 25.8°$ which corresponds to (011) reflections of the wurtzite (hexagonal) phase of PbI$_2$ according to the standard database ASTM (ICSD, 01-079-0803). Other lines accompanying the reflections belong to (001), (102), (003), (110), and (004) which correspond with $2\theta = 12.6°$, $34.1°$, $38.4°$, $39.5°$, $52.4°$, respectively [12]. PbI$_2$ is a hexagonal semiconductor material with lattice constants of $a = 4.562$ Å and $c = 6.985$ Å [13].

SEM of Pb$_{1-x}$Zn$_x$I$_2$

The SEM of Pb$_{1-x}$Zn$_x$I$_2$ nanostructures revealed the formation of hexagonal platelets and rods grown on the substrate as well as grains and voids. The morphology of the grain is mostly of closely irregular platelets and rods. Figure 2 shows that the grain size of Pb$_{1-x}$Zn$_x$I$_2$ is not affected by increasing Zn doping which is consistent with the XRD results.

Fig. 1 XRD patterns of purified PbI$_2$ materials

Fig. 2 SEM image spectra of Pb$_{1-x}$Zn$_x$I$_2$ nanostructures with various Zn moles fractions *x* **a** $x = 0.02$, **b** $x = 0.04$, **c** $x = 0.06$, and **d** $x = 0.08$

Metal–semiconductor–metal photodetector-based on PbI$_2$

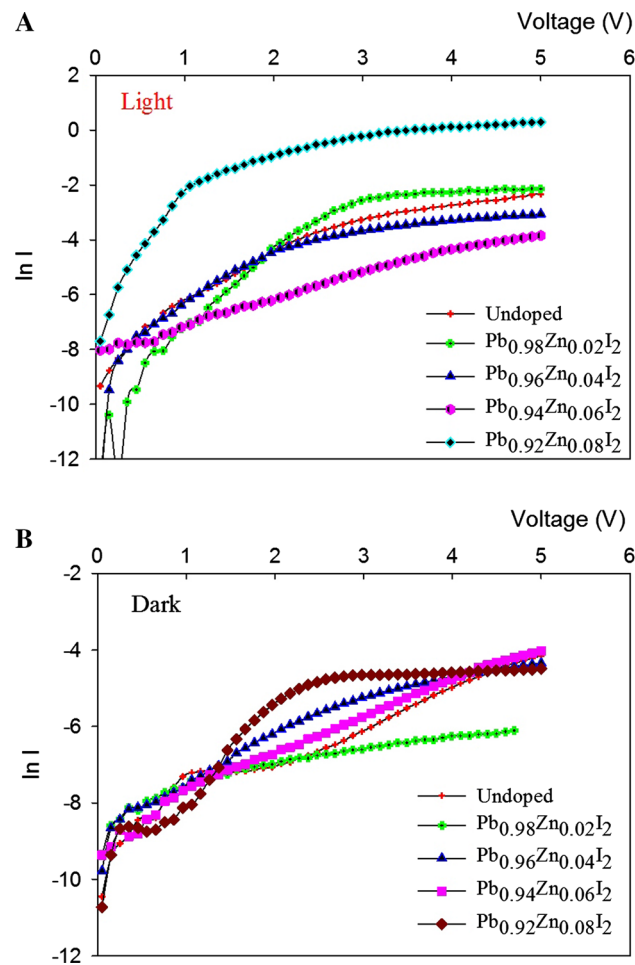The following subsections present the characterizations of the fabricated device.

Electrical measurements of Ag-based Schottky contact

Figure 3 shows the plot of ln I as a function of voltage to calculate the barrier height for Ag contact on PbI$_2$ and Pb$_{0.92}$Zn$_{0.08}$I$_2$.

Figure 4 shows the I–V characteristics from -6 to 6 V of the PbI$_2$ and Pb$_{1-x}$Zn$_x$I$_2$ measured in the dark and white light (tungsten lamp) and under 460 nm. Figure 4 shows the current–voltage (I–V) characteristics of Ag-based Schottky contact for (a) PbI$_2$ and (b, c, d, and e) doped Pb$_{1-x}$Zn$_x$I$_2$, respectively. The Schottky barrier heights (SBH) and ideality factor of these contacts were calculated through the I–V measurements using equations

$$I = I_\circ \exp\left(\frac{qV}{nK_BT}\right) \text{ and } I_\circ = A^*AT^2 \exp\left(\frac{-q\phi_B}{K_BT}\right)$$

where $I_\circ$ is the saturation current, n is the ideality factor, K_B is the Boltzmann's constant, T is the absolute temperature, A^* is the effective Richardson coefficient, A is the area of the Schottky contact, and Φ_B is the barrier height. The leakage current value was determined at (2 V). It can be seen from Fig. 4b that the curves show a rectifying behavior and this improved with doped, indicating that the addition of 0.02 Zn to PbI$_2$ produces a strong chemical reaction and better contact. Ag metal contact has a high work function (4.70 eV) [14]. As a result, (b) shows the highest Schottky barrier value compared with the rates of other zinc. This indicates that it has good surface morphology. The mechanism to change the value of current at higher electric fields depends on changing the energy gap. The Schottky barrier height SBH and ideality factor are summarized in Table 1.

Photocurrent response of Pb$_{0.98}$Zn$_{0.02}$I$_2$ device

The light responsivity (R) of Pb$_{0.98}$Zn$_{0.02}$I$_2$ was calculated using equation

$$R = \frac{I_{Ph}}{AP_{opt}}$$

where I_{ph} is the photocurrent, A is the illuminated area, and p_{opt} is the power of the incident light.

Figure 5 shows a plot of the responsivity against the wavelength (under bias voltage of 3 V). As shown in Fig. 5, the highest R-value was observed at 460 nm. The photocurrent response of the Pb$_{0.98}$Zn$_{0.02}$I$_2$ device was studied at various bias voltages under illumination with 460-nm chopped light. Figure 6 shows the photocurrent response curves at applied bias voltages of 1, 3, and 5. The current was increased to saturation when it was illuminated and decreased again when the light was switched off. When the device is illuminated with sufficient energy, electron–hole pairs are formed by optical absorption. These pairs are separated under the applied electrical field at the Zn–PbI$_2$ interface. The rise time of the device exposed to 460-nm light ranged from 53 to 61 ms and the fall time from 57 to 63 ms depending on the bias voltage. Table 1 lists the rise time and decay time in Fig. 7. The sensitivity of the fabricated device was determined at a different applied bias voltage using equation $S = \frac{I_{Light} - I_{Dark}}{I_{Dark}} \times 100\%$, and the device was more sensitive to 460 nm light than to illumination at other wavelengths. At b bias voltage of 3 V, the sensitivity of the device under 460-nm light was 5472% as shown in Table 2. Quantum efficiency (η) is an important parameter to evaluate the performance of the photosensitive device. It is related to the

Fig. 3 Plot of voltage as a function of ln I to calculate the barrier height for Ag contact on undoped and doped under **a** illumination and **b** dark conditions
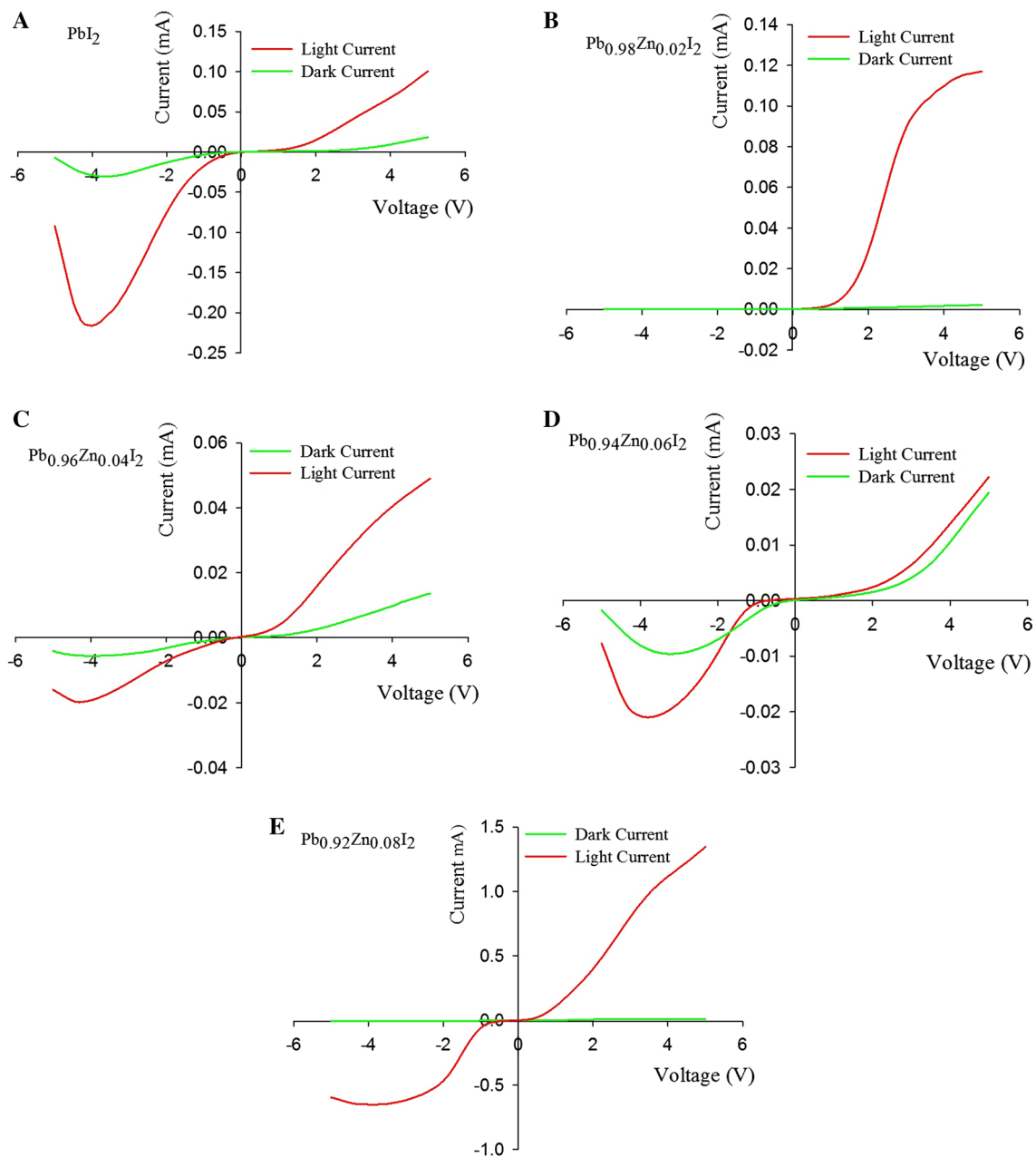
Fig. 4 *I–V* characteristics of Ag-Schottky contact with **a** PbI_2, (**b–e**) $Pb_{1-x}Zn_xI_2$ nanostructures

number of electron–hole pairs excited by absorbed photons as given by equation
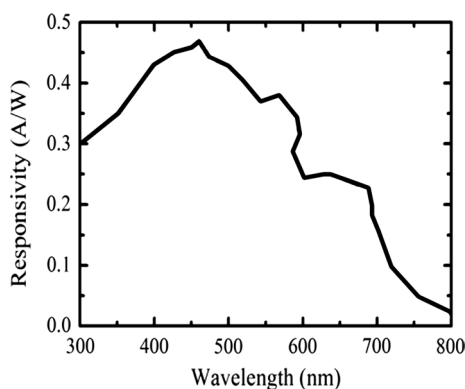
$$\eta = \frac{hc}{e\lambda} R_\lambda$$

where h is Planck's constant, c is the speed of light, e is the electron charge, λ is the wavelength, and R_λ is the spectral responsivity. The efficiency (η) values of the fabricated $Pb_{0.98}Zn_{0.02}I_2$ detector were found to be dependent on the bias voltage and the wavelength of the incident light as shown in Table 2. The high quantum efficiency of $Pb_{0.98}Zn_{0.02}I_2$ photodetector is related to the large value of the carrier mobility lifetime.

Table 1 Structural and electrical properties of PbI_2 and $Pb_{1-x}Zn_xI_2$ nanostructure
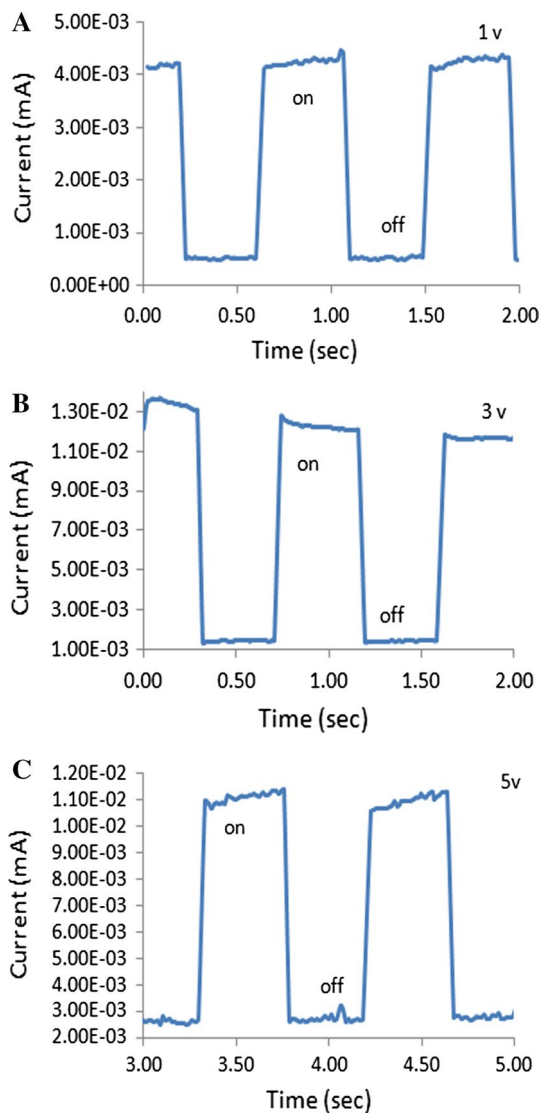
Sample	Ideality factor (n)	Barrier height (eV)	Leakage current
Undoped PbI_2			
Light	1.7	0.64	$-7.967657E-05$
Dark	2.6	0.67	$-1.369305E-05$
$Pb_{0.98}Zn_{0.02}I_2$			
Light	1.6	0.84	$-5.202599E-08$
Dark	1.08	0.83	$-5.380798E-09$
$Pb_{0.96}Zn_{0.04}I_2$			
Light	2.1	0.76	$-2.046658E-04$
Dark	6	0.79	$-3.346693E-06$
$Pb_{0.94}Zn_{0.06}I_2$			
Light	3.6	0.40	$-1.053405E-05$
Dark	1.2	0.64	$-7.373940E-06$
$Pb_{0.92}Zn_{0.08}I_2$			
Light	2.6	0.64	$-4.969795E-04$
Dark	3.9	0.68	$-2.677603E-06$

Fig. 5 Light responsivity versus wavelengths of light fabricated poly-crystalline PbI_2 photodetector

Fig. 6 Photoresponse of $Pb_{0.98}Zn_{0.02}I_2$ device illuminated by chopped 460-nm light at various bias voltages **a** 1 V, **b** 3 V, and **c** 5 V

Conclusions

Thin-film samples of doped Zn–PbI_2 with different weights of zinc dopants on glass substrate were prepared successfully. The Ag-based Schottky contacts based on PbI_2 and $Pb_{1-x}Zn_xI_2$ nanostructures have been investigated. All the samples revealed a variable behavior, and they become more rectifying when adding Zn impurity with good electrical properties of $Pb_{0.98}Zn_{0.02}I_2$. Good results for SBH have been obtained at $Pb_{0.98}Zn_{0.02}I_2$ due to good structural and electrical properties for this sample. In addition, the surface

Fig. 7 Scheme to clarify the calculation of rise time and decay time

Table 2 Photoelectrical parameters of $Pb_{0.98}Zn_{0.02}I_2$ photodetector device

Sample	Wavelength (nm)	Bias voltage (V)	Rise time (ms)	Decay time (ms)	Sensitivity (%)	Quantum efficiency (η) (%) ($\times 10^2$)
$Pb_{0.98}Zn_{0.02}I_2$	460	1	61	63	2890.656	2.95
		3	53	57	5472.738	9.19
		5	57	59	583.9345	6.80

morphology plays an important role in the interface between the metal and Zn–PbI_2 surface, which in turn reduces tunneling effect and increases the thermionic emission which, eventually, leads to improving the Schottky barrier height.

Open Access This article is distributed under the terms of the Creative Commons Attribution 4.0 International License (http://creativecommons.org/licenses/by/4.0/), which permits unrestricted use, distribution, and reproduction in any medium, provided you give appropriate credit to the original author(s) and the source, provide a link to the Creative Commons license, and indicate if changes were made.

References

1. Shah, K.S., et al.: Electronic noise in lead iodide x-ray detectors. Nucl. Inst. Methods Phys. Res. **353**, 85–88 (1994)
2. Ponpon, J.P., Amann, M.: Preliminary characterization of PbI_2 polycrystalline layers deposited from solution for nuclear detector applications. Thin Solid Films **394**, 277–283 (2001)
3. Yanga, C.H., Yaua, S.L., Fanb, L.J., Yang, Y.W.: Deposition of lead iodide films on Rh(100) electrodes from colloidal solutions—the effect of an iodine adlayer. Surf. Sci. **540**, 274–284 (2003)
4. Bhavsar, D.S., Saraf, K.B.: Optical and structural properties of Zn-doped lead iodide thin films. Mater. Chem. Phys. **78**, 630–636 (2003)
5. Verma, K.C., et al.: Lattice defect-formulated ferromagnetism and UV photo-response in pure and Nd, Sm substituted ZnO thin films. Phys. Chem. Chem. Phys. **21**, 12540–12554 (2019)
6. Lam, K.-T., et al.: High-sensitive ultraviolet photodetectors based on ZnO nanorods/CdS heterostructures. Nanoscale Res. Lett. **12**, 31 (2017)
7. Bhardwaj, R., et al.: Structural and electronic investigation of ZnO nanostructures synthesized under different environments. Heliyon **4**, e00594 (2018)
8. Dawood, R.I., Froty, A.J.: The formation of photographic images in single crystals of lead iodide. J. Theor. Exp. Appl. Phys. **5**, 1003–1008 (1960)
9. Dmitruk, N.L., Shari, V.M., Kostyshin, M.T., Mikhailovskaya, E.V.: Sov. Phys. Semicond. **14**, 350 (1980)
10. Fornaro, L., Saucedo, E., Mussio, L., Gancharov, A.: IEEE Trans. Nucl. Sci. **49**, 3300 (2002)
11. Shah, K., Street, R., Dmitriyev, Y., Bennett, P., Cirignano, L., Klugerman, M., Squillante, M., Entine, G.: X-ray imaging with PbI_2 based a Si:H flat panel detectors. Nucl. Instrum. Methods Phys. Res. A **458**, 140–147 (2001)
12. Deich, V., Roth, M.: Improved performance lead iodide nuclear radiation detectors. Nucl. Instrum. Methods Phys. Res., Sect. A **380**(1–2), 169–172 (1996)
13. Dollahon, N., Gopi, K.K., Ahmadi, T.: Fabrication and characterization of solid PbI_2 nanocrystals. J. Phys. D Appl. Phys. **40**(6), 1778–1783 (2007)
14. Hong, J.-P., Park, A.-Y., Lee, S., Kang, J., Shin, N., Yoon, D.Y.: Tuning of Ag work functions by self-assembled monolayers of aromatic thiols for an efficient hole injection for solution processed triisopropylsilylethynyl pentacene organic thin film transistors. Appl. Phys. Lett. **92**(14), 143311–143313 (2008)

Publisher's Note Springer Nature remains neutral with regard to jurisdictional claims in published maps and institutional affiliations.